Reconstructing of a Non-Minimum Phase Response from Far-Field Power Pattern of an Electromagnetic System

Jie Yang and Tapan K. Sarkar
Department of Electrical Computer Engineering
121 Link Hall, Syracuse University, New York 13244, USA
Email: jyang14@syr.edu, tksarkar@syr.edu

Abstract: A new technique for reconstructing the non-minimum phase function from magnitude-only data is presented in this paper. The non-minimum phase is reconstructed by utilizing the fact that the DFT of the square of magnitude response is equal to the auto-correlation of time domain sequence. An all-pass filter representation is also used to reduce the computational load. This approach is applied to the synthesis of non-minimum phase functions from the magnitude only antenna pattern. Several examples dealing with a single antenna and antenna arrays are simulated to illustrate the applicability of this approach.

Keywords: Phase Reconstruction, Non-minimum Phase, Magnitude-only Data

1. Introduction

In electromagnetic system, the magnitude response can easily be measured but the phase response is hard to obtain. Therefore it is important to reconstruct the phase response from amplitude-only data. For a minimum phase system, if the signal is causal, i.e., $x(t) = 0$ when $t < 0$, the phase reconstruction from amplitude-only data is relatively straightforward by applying Cepstrum analysis [1]-[2]. It can be shown that the minimum phase is the Hilbert transform of the log magnitude of the amplitude, which can be expressed as:

$$\arg[X(\omega)] = H[\log(|X(\omega)|)] \tag{1}$$

where $H[\cdot]$ denotes the Hilbert transform. The minimum phase property of a transfer function $X(\omega)$ refers to the zeros of $X(\omega)$ which are all inside the unit circle of the *z*-plane ($z = e^{\sigma + j\omega}$ with $|z| < 1$) or in the left half of the *s*-plane ($s = \sigma + j\omega$ with $\sigma < 0$). If the system is not a minimum-phase system, Equation (1) doesn't hold. Since most electromagnetic systems are distributed and have a non-minimum phase response, the Cepstrum method given by Equation (1) is not much useful for practical non-minimum phase reconstruction. In previous researches, the principle of causality in time domain has been used to realize the phase reconstruction [3]. Meanwhile, the discrete cosine transform and the all-pass filter representation have been used to reduce the computation load when the amplitude data is symmetric [4]. In the current approach, the discrete Fourier transform instead of the cosine transform is utilized to expend the ability of dealing with the non-symmetric amplitude data. It is important to emphasize that the phase reconstruction is not a unique problem, because the addition of a linear phase difference to the actual phase response is equivalent to a pure delay in the time domain. Since we are dealing with LTI (linear time-invariant) system, changing the impulse response of the system by a time shift does not change the transfer function of the original system except that the phase spectrum is modified by a linear phase function, and the amplitude spectrum is unchanged. The slope of the linear phase difference corresponds to the time delay.

In Section 2, we describe the computational method and a detailed derivation, as to how this approach can be used to reconstruct the non-minimum phase response from the power radiation pattern. Some numerical examples are presented in Section 3, followed by the conclusion in Section 4.

2. Approach

For a causal sequence x_n where $n = 1, 2, ..., N$, its frequency response in the Fourier transform domain, $X(\omega)$, can be obtained by using the following Fourier transform:

$$X(\omega) = \sum_{n=0}^{\infty} x_n e^{-j\omega n} \tag{2}$$

The magnitude square of the frequency response, i.e., the power spectrum, can be written as:

$$|X(\omega)|^2 = X(\omega)X^*(\omega) = \sum_{n=0}^{\infty} x_n e^{-j\omega n} \sum_{m=0}^{\infty} x_m^* e^{-j\omega m} = \sum_{n=0}^{\infty}\sum_{m=0}^{\infty} x_n e^{-j\omega n} x_m^* e^{-j\omega m} = \sum_{n=0}^{\infty}\sum_{m=0}^{\infty} x_n x_m^* e^{j(m-n)\omega} \tag{3}$$

where $X^*(\omega)$ is the complex conjugate of $X(\omega)$. Multiply both sides by $e^{-jk\omega}$ (where k is an integer) and integrate from 0 to 2π . This results in:

$$\begin{aligned} \int_0^{2\pi} |X(\omega)|^2 \, e^{-jk\omega} d\omega &= \int_0^{2\pi} \sum_{n=0}^{\infty}\sum_{m=0}^{\infty} x_n x_m^* e^{j(m-n-k)\omega} d\omega = \sum_{n=0}^{\infty}\sum_{m=0}^{\infty} x_n x_m^* \int_0^{2\pi} e^{j(m-n-k)\omega} d\omega \\ &= 2\pi \sum_{n=0}^{\infty}\sum_{m=0}^{\infty} x_n x_m^* \ (k = m - n) = 2\pi \sum_{n=0}^{\infty} x_n x_{n+k}^* \end{aligned} \tag{4}$$

Since we are not dealing with the continuous magnitude response but with a finite number N of the amplitude data, Equation (4) need to be written in the discrete form as:

$$\Delta\omega \sum_{i=0}^{N} |X(\omega_i)|^2 \, e^{-jk\omega_i} = 2\pi \sum_{n=0}^{N} x_n x_{n+k}^* \tag{5}$$

where $\Delta\omega$ is the frequency interval and $X(\omega_i)$ is the discrete Fourier transform of sequence x_n .
The left hand side of Equation (5) is the DFT of the magnitude response and the right hand side is the autocorrelation of the time domain sequence. The last half of sequence x_n , which corresponds to the negative index of *n*, should be filled with 0 to satisfy the causality condition, otherwise Equation (8) will not hold. An error function is now defined, the minimization of which leads to the x_n from the power pattern. The error function is:

$$Error(x_n) = \left| \Delta\omega \sum_{i=0}^{N} |X(\omega_i)|^2 \, e^{-jk\omega_i} - 2\pi \sum_{n=0}^{N} x_n x'_{n+k} \right| \tag{6}$$

The time domain sequence x_n can be solved by minimizing the error function, from which the desired phase response can be solved by Equation (2). Note that for a delayed version of x_n , as long as it is causal, the autocorrelation in Equation (6) will yield the same result, therefore the solution is not unique. The non-uniqueness of the solution will cause a linear phase difference in the frequency domain. As in general x_n is complex, optimization of Equation (6) requires a 2*N* dimensional searching over x_n , so the computational load can be very large. We can use an all-pass filter representation to reduce the computational load, as shown next.
The actual frequency response can be represented by the product of the minimum frequency response and the frequency response of an all-pass filter, that is:

$$X(\omega) = X_{\min}(\omega) H_{\text{all-pass}}(\omega) = |X(\omega)| \, e^{jH[\log|X(\omega)|]} H_{\text{all-pass}}(\omega) \tag{7}$$

The frequency response $H_{\text{all-pass}}(\omega)$ can be represented in terms of the following pole-zero factorization:

$$H_{\text{all-pass}}(\omega) = \prod_{p=0}^{P-1} \frac{e^{-j\omega} - a_p}{1 - a_p e^{-j\omega}} \prod_{q=0}^{Q-1} \frac{\left(e^{-j\omega} - b_q\right)\left(e^{-j\omega} - b_q^*\right)}{\left(1 - b_q e^{-j\omega}\right)\left(1 - b_q^* e^{-j\omega}\right)} \tag{8}$$

where a_p and b_q are the real and complex pole-zeros of the all-pass filter respectively. Rewriting Equation (6) as the function of a_p and b_q, one can redefine the error function as:

$$Error(a_p, b_q) = \left| \Delta\omega \sum_{i=0}^{N} |X(\omega_i)|^2 e^{-jk\omega_i} - 2\pi C\left\{ IFT\left[X_{\min}(\omega) H_{\text{all-pass}}(\omega) \right] \right\} \right| \tag{9}$$

where $C(x_n) = \sum_{n=0}^{N} x_n x_{n+k}^*$, and $IFT(\cdot)$ denotes an inverse Fourier transform. Equation (9) has only $P+2Q$ variables, so the computational load is significantly reduced from a 20-30 dimensional search [2] to a 3-6 dimensional search (P and Q are 1 or 2) to minimize the error. Because it is very hard to get the gradient of variables a_p and b_q, the down-hill simplex in multi-dimension method [5] is used to optimize the solution. After the parameters a_p and b_q are estimated, the desired phase response is given by Equation (7).

For the electromagnetic system, the radiation electric field is proportional to the Fourier transform of the current distribution on the electromagnetic structure. If we assume a current directed in the $\hat{z}$ direction, then the far field can be expressed as [6]:

$$\vec{E} = j\omega\vec{A} = j\omega \frac{e^{-jkr}}{4\pi r} \int dx \int dy \int dz J_z(x,y,z) e^{jk(x\sin\theta\sin\phi + y\sin\theta\cos\phi + z\cos\theta)} \tag{10}$$

where $\vec{A}$ is the magnetic vector potential, $k = 2\pi/\lambda$ and r is the spatial far-field variable. If we further restrict the current distribution in $y = 0$ plane and measure the far-field at $\phi = 0$, Equation (10) can be simplified to:

$$\vec{E} = j\omega \frac{e^{-jkr}}{4\pi r} \int dx \int dz J_z(x,z) e^{jkz\cos\theta} = j\omega \frac{e^{-jkr}}{4\pi r} \int dx \int dz J_z(x,z) e^{jkzu} \tag{11}$$

where $u = \cos\theta$. Equation (11) indicates that the far-field is proportional to the Fourier transform of the current distribution with the variable changed from θ to $\cos\theta$. Since all antennas are of finite length, it is appropriate to claim that the spatial current distribution is causal. So we can apply the above approach to reconstruct the phase response based on the far-field power pattern of the electromagnetic system.

Since in general the far-field amplitude data is equally distributed in θ space, it is necessary to interpolate $E(\theta)\,(\theta = 0, 1^\circ, \ldots 180^\circ)$ to $E(u)\,(u = -1, \ldots 0, 1/N, 2/N, \ldots 1)$, so that the fast Fourier transform can still be used [7]. Because of the variation of $\cos\theta$, we can only get the data in the region $u \in [-1,1]$. However we need the data for $u \in [-\infty, \infty]$ (normally the data in the range of $u \in [-10,10]$ is long enough). For large value of u, the fields in the invisible region are set to 0 [3]. After interpolation and padding with zeros, we can use Equation (9) to perform an optimization. Also we need to point out that the $u \in [-1,1]$ corresponding to the original data, so the optimization is performed only for this region.

In the numerical examples presented in the next section, we use the linear regression to check the linearity of the phase difference between the actual phase and the estimated phase and compare it with the minimum phase response to verify that the minimum phase function does not provide the correct solution for non-minimum phase system. The error of estimation s, which is the square root of the residual variance, is given by:

$$s = \sqrt{\sum_{i=1}^{N} r_i^2 / (N-2)} \tag{12}$$

where r_i is the residual at each point and N is the number of data.

3. Numerical Examples

In this section we provide several numerical examples of the far-field phase reconstruction, including both single antennas and antenna arrays. The actual amplitude and phase data are all generated by using the computer software WIPL-D [8]. Also, for each example, one real pole-zero and two complex pole-zeros ($P = 1, Q = 2$) are used in the all-pass characterization. The data obtained from WIPL-D are interpolated in the u space ($u \in [-1,1]$) and extrapolated to the region $u \in [-10,10]$ by padding it up with zeros. All the figures in this section are based on $u = \cos\theta$ instead of θ.

For the first example, consider a horn antenna shown in Figure 1. The probe at the end of the horn excited with 1 volt at frequency 2.3GHz and is oriented along z axis and the length is 40mm. The dimensions of the horn antenna are: a_1=72mm, b_1=80mm, c_1=50mm, a_2=60mm, b_2=30mm, c_2=50mm and d=25mm. The far-field power pattern is given in Figure 2. Figure 3(a) shows the actual phase (solid line), the minimum phase (dotted line) and the estimated phase (dashed line) responses for the horn antenna, and Figure 3(b) gives the phase difference between actual and estimated phase (dashed line), and difference between the actual phase and the minimum phase (dotted line). The standard error of estimation for the estimated phase and the minimum phase are 4.1 and 41.9 respectively. From Figure 3(b) we can see that the minimum phase is nowhere near the desired solution, but the estimated phase provides a good estimation to the actual phase function, and the difference between the actual phase function and the computed phase function is approximately linear.

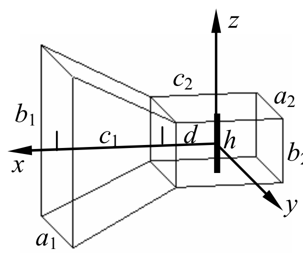

Figure 1. Horn Antenna

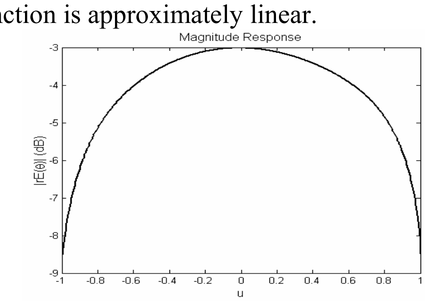

Figure 2. Magnitude Response of the Horn Antenna

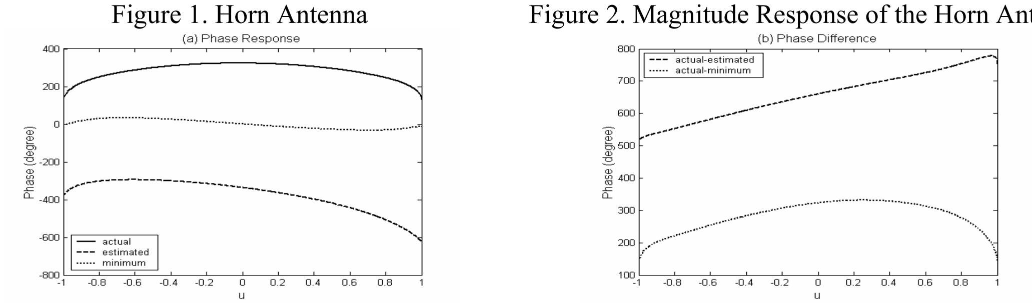

Figure 3. Actual, Minimum and Estimated Phase Responses of the Horn Antenna

For the second example, consider a microstrip patch antenna as shown in Figure 4. The probe is connected to a long rectangular metallic strip and a square patch which are printed over the dielectric substrate with ε_r=2.6. The dimension of the patch and the substrate are given as: a_1=76.56mm, b_1=48.72mm, a_2=b_2=34.8mm, a_3=34.8, b_3=7.36mm, h_1=1.575mm, h_2=0.4725mm. The excitation is 1 volt and the frequency is 2.6GHz. The far-field power pattern is given in Figure 5. Similar to the first example, the phase responses and phase differences are plotted in Figure 6. The error for the estimated phase and the minimum phase are 1.1 and 5.1 respectively. From figure 6(b), the difference between the actual phase and the estimated phase is more linear than the difference between the actual phase and the minimum phase.

Next we deal Antenna Arrays. For the third example, consider an array of horn antenna as shown in Figure 7. There are 11 elements in this array equally spaced along z direction and each element is identical to the horn antenna of example 1. The distance between any two elements is one wavelength. All generators are excited simultaneously. The far-field power pattern is given in Figure 8, and the phase responses and the phase differences are plotted in Figure 9. The error with the estimated phase and the minimum phase are 97.8 and 171.7 respectively. These values are relatively large because there are a couple of glitches in Figure 9(b) which occur at the power pattern minimums where the magnitude data are so small that the phase reconstruction at these points becomes inaccurate. But the reconstructed phase function between two glitches is pretty linear, and the overall phase difference between the reconstructed phase function and the actual phase is approximately a straight line.

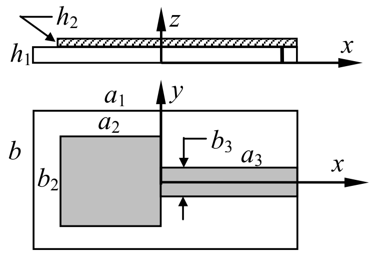

Figure 4. Microstrip Patch Antenna

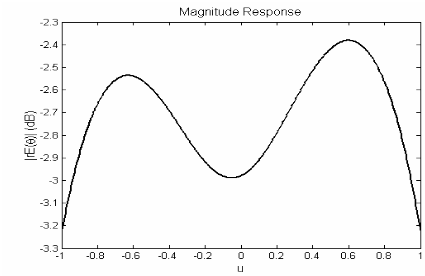

Figure 5. Magnitude Response of the Patch Antenna

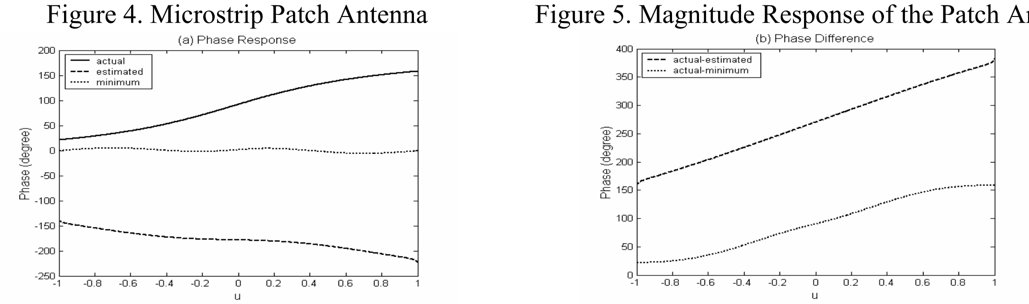

Figure 6. Actual, Minimum and Estimated Phase Responses of the Patch Antenna

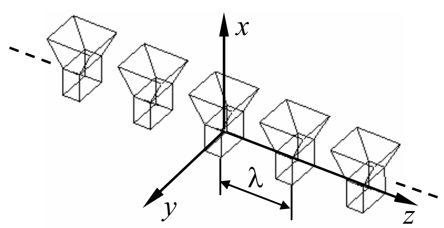

Figure 7. Horn Antenna Array

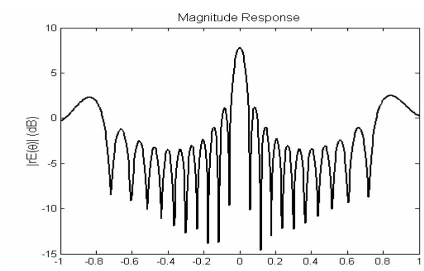

Figure 8. Magnitude Response of the Horn Array

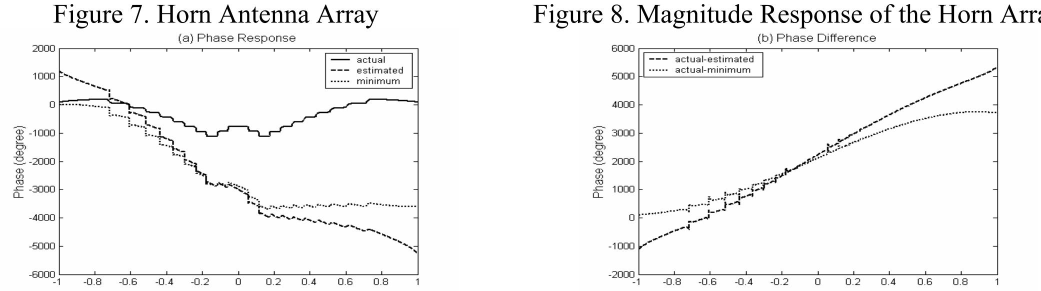

Figure 9. Actual, Minimum and Estimated Phase Responses of the Horn Antenna Array

As the last example, consider the power pattern from a Yagi antenna. The structure of the Yagi antenna is plotted in Figure 10. There are 24 elements in 2 groups along the *y* direction. One group is above the *x-o-y* plane, the other is below the *x-o-y* plane. The length of driven element l_1=358.758mm, and the length of the director l_2=234.462mm, the distance between driven element and the director d_1=173.609m, the distance between the two groups d_2=343.7mm, the distance between elements in each group d=371.3mm, and a=116.708mm. The driven elements were fed at the center with 1 volt excitation at 450MHz. The far-field power pattern is shown in Figure 11. The phase response and the phase differences are given in Figure 12. The error for the estimated phase and the minimum phase are 29.4 and 103.9 respectively. From Figure 12(b) we can see that the difference between the estimated phase and the actual phase is almost a straight line, where the difference between the minimum phase and the actual phase is a curved line.

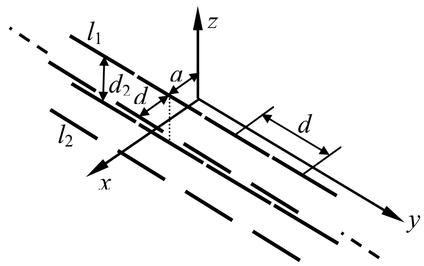

Figure 10. Yagi Antenna

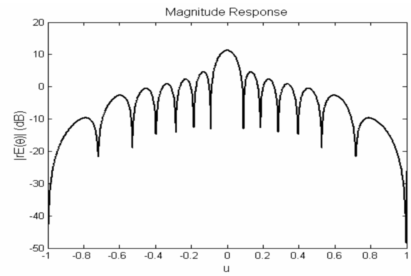

Figure 11. Magnitude Response of the Yagi Antenna

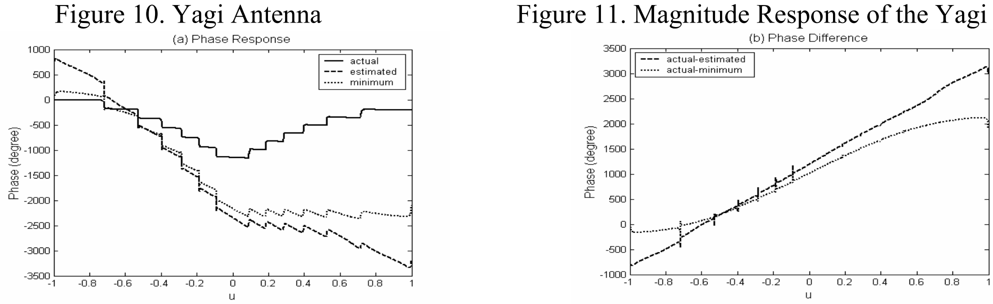

Figure 12. Actual, Minimum and Estimated Phase Responses of the Yagi Antenna

4. Conclusion

A method based on the equality between DFT of the far field power pattern and the auto-correlation of equivalent current sequence is defined to generate the non-minimum phase response from an amplitude response of an electromagnetic system. The all-pass filter representation is also utilized for more efficient computation. In all the numerical examples, 5 coefficients has been used to model the all-pass filter of the optimization process, and the differences between the estimated phase response and the actual phase response are close to being linear.

References

[1] A. V. Oppenheim and R. W. Schafer, *Discrete-time Signal Processing*, 2nd ed. Prentice Hall, Englewood Cliffs, New Jersey, 1989.

[2] M. H. Hayes, “The reconstruction of a multidimensional sequence from the phase or magnitude of its Fourier transform”. *IEEE Trans. Acoust. Speech. Signal Processing*, Vol. ASSP-30, pp. 140-145, 1982.

[3] T. K. Sarkar and B. Hu, “Generation of nonminimum phase from amplitude only data”, *IEEE Trans MTT*, Vol. 46, No. 3, pp. 1079-1084, 1998.

[4] J. Koh, Y. K. Cho and T. K. Sarkar, Reconstruction of non-minimum phase function from only amplitude data, Microwave and Optical Technology Letters, Vol. 35 No. 3, pp. 212-216, 2002.

[5] W. H. Press *et al*., *Numerical Recipes*, 2nd ed. Cambridge University Press, 1992.

[6] W. L. Stulzman and G.A. Thiele, *Antenna Theory and Design*, Wiley, New York, 1981.

[7] S. Narayana *et al*., “A comparision of two techniques for the interpolation extrapolation of frequency domain responses”, Digital signal Processing, Vol. 6, pp. 51-67, 1966.

[8] B. Kolundzija *et al*., *WIPL-D: Electromagnetic Modeling of Composite Metallic and Dielectric Structures - Software and User's Manual*, Artech House, 2000.

